Electrocatalysis

Potential-Induced Surface Restructuring—The Need for Structural Characterization in Electrocatalysis Research**

Albert K. Engstfeld, Sylvain Brimaud, and R. Jürgen Behm

Abstract: The necessity of the careful structural character-ization of model electrodes before and after the electrochem-ical measurements for a proper mechanistic interpretation is demonstrated for a well-known electrocatalytic system, bulk CO oxidation on PtRu model electrodes. Bimetallic, Pt-monolayer-island-modified Ru(0001) electrodes, which were prepared and characterized by scanning tunneling microscopy under ultrahigh-vacuum conditions, were found to undergo a distinct restructuring when they were potential cycled to 1.05 V_{RHE}, while up to 0.90 V_{RHE} they are stable. The restruc-turing, which is not evident in base voltammograms, is accompanied by a significant increase in the CO oxidation activity at low potentials (0.5–0.8 V), indicating that it is caused by new active sites created by the restructuring, and not by the PtRu sites that existed in the original surface and that were previously held responsible for the high activity of these bimetallic surfaces in terms of a bifunctional mechanism.

$\mathbf{M}$odel studies performed on single-crystal electrodes are indispensable for a detailed mechanistic understanding of electrocatalytic reactions, since they allow measurements on structurally well-defined (and tunable) surfaces and thus structure–reactivity correlations can be mapped out.[1] Fur-thermore, they provide a perfect basis for comparison with theory. The prerequisite for the mechanistic interpretation, however, is detailed knowledge of the actual surface struc-ture, both before and, even more importantly, during/after the electrocatalytic reaction. Even small structural rearrange-ments, which may be hardly detectable by electrochemical characterization, for example by potential cycling in a sup-porting electrolyte, may significantly modify the electrocata-lytic properties of the surface by providing (or destroying) highly active sites.[2,3] This is particularly important for electrode surfaces that tend to be structurally or chemically unstable under reaction conditions.

In the present communication we illustrate the necessity of proper structural characterization of the electrode and of the structural changes induced by the electrochemical/elec-trocatalytic reaction for the unambiguous mechanistic inter-pretation of the electrocatalytic reaction, using the oxidation of CO on bimetallic PtRu electrodes as an example. PtRu electrodes/catalysts are among the most well known and most intensely studied bimetallic systems in electrocatalysis[4] because of their high activity in the oxidation of methanol and CO and, as a result of the latter, their high CO tolerance in the oxidation of H_2 feeds contaminated by trace impurities of CO. This makes them highly attractive as anode catalysts in polymer electrolyte membrane fuel cells (PEMFCs) operated with CO-containing H_2 feed gases and also in direct methanol fuel cells (DMFCs).[5,6] Already in 1975, the high activity of PtRu in these reactions was explained by a bifunctional mechanism, where Ru atoms supply adsorbed OH at lower potential than Pt, which then reacts with CO adsorbed on adjacent Pt sites.[7]

Using scanning tunneling microscopy (STM) for struc-tural characterization before and after the electrochemical measurements, and a flow cell system for bulk CO electro-oxidation measurements, we demonstrate that previous results obtained on single-crystal PtRu model systems were strongly affected by restructuring processes during the electrochemical/electrocatalytic measurements, and that the actual mechanism for CO oxidation is significantly more complex than previously thought. The measurements were performed in a novel combined ultrahigh-vacuum (UHV) STM electrochemistry (EC) system, which allowed STM measurements before and after the electrochemical measure-ments and controlled transfer between the UHV and the electrochemical cell. We investigated Pt-modified Ru(0001) electrodes with monolayer-thick islands and PtRu monolayer surface alloys on Ru(0001) with similar Pt surface content, which were prepared and characterized under UHV condi-tions prior to the electrochemical measurements.

Structural modifications will first be illustrated for the Pt-free Ru(0001) substrate. Cyclic voltammograms (CVs) of a UHV-prepared Ru(0001) electrode, recorded in 0.5 M H_2SO_4, where the upper potential limit was stepwise increased, are displayed in Figure 1a. They largely resemble previously published data.[8–10] A distinct oxidation peak at 0.64 V (P1, followed by a shoulder at higher potential) and two reduction peaks at 0.52 V (P2) and 0.32 V (P3) are resolved. Coulometric analysis of the anodic and cathodic

[*] A. K. Engstfeld,[+] Dr. S. Brimaud,[+] Prof. Dr. R. J. Behm
Institute of Surface Chemistry and Catalysis, Ulm University
Albert-Einstein-Allee 47, 89081 Ulm (Germany)
E-mail: juergen.behm@uni-ulm.de
Homepage: http://www.uni-ulm.de/nawi/iok.html

[+] These authors contributed equally to this work.

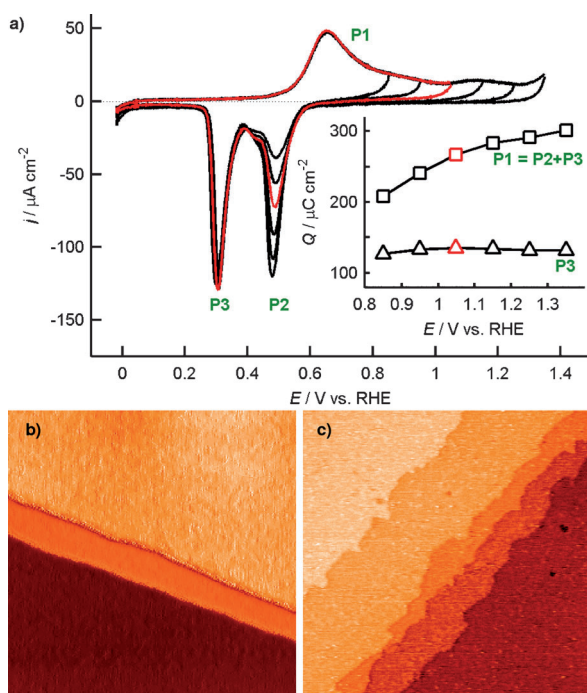Supporting information for this article (details of experiments and the combined UHV–STM–EC system) is available on the WWW under http://dx.doi.org/10.1002/anie.201404479.

Figure 1. a) CV of Ru(0001) recorded at 50 mVs^{-1} in 0.5 M H$_2$SO$_4$ with increased upper potential limit. The insert shows the evolution of the charge under the oxidation peak P1 which is equal to the sum of the charges under the reduction peaks P2 + P3, and of the charge under the peak P3 alone, which is correlated with the Pt-free Ru(0001) areas. b,c) STM images (200 nm × 200 nm) of a bare UHV-prepared Ru(0001) electrode (b) and of the same electrode after repeated potential cycling up to 0.90 V (c).

Figure 2. a) CV recorded at 10 mVs^{-1} and in 0.5 M H$_2$SO$_4$ for Ru(0001) (black, dashed line), 0.32 ML Pt/Ru(0001) (blue dotted line), and 0.40 ML Pt/Ru(0001) (red line). The inset shows an STM image (200 nm × 200 nm) of a 0.32 ML Pt modified Ru(0001) electrode directly after preparation. b,c) STM images (200 nm × 200 nm) of the electrode after potential cycling up to 0.9 V (b) and 1.05 V (c).

potential scans (see inset) demonstrates the reversibility of the surface redox processes. A detailed analysis of the CV and the minor changes apparent in the peak positions, the shoulder of the reduction peak at 0.40 V, and in the hydrogen region can be found in the Supporting Information.

STM imaging indicates that prior to the electrochemical measurements, the freshly prepared Ru(0001) surface has extended atomically smooth terraces separated by mainly monolayer steps with straight edges (Figure 1 b), while after potential cycling up to 0.90 V, we find clear indications of step edge corrosion, with rough step edges (Figure 1 c). Comparable findings, with an onset of Ru(0001) oxidation at the step edges, was also reported by Vukmirovic et al. from in situ STM measurements, together with the formation of RuO$_2$ clusters at higher potentials.[11]

From these images it is not clear whether the surface corrosion was limited to step roughening (by transport on the surface) or whether it involves dissolution of surface Ru atoms from the step edges into the electrolyte (and possible redeposition). It will become more clear from images recorded on bimetallic surfaces with Pt deposits on top of the Ru(0001) substrate that the latter is much more likely (Figures 2 and 4).

It is important to realize that the increasing number of Ru step sites, clearly evident from STM imaging (see Figure 1 b,c), does not lead to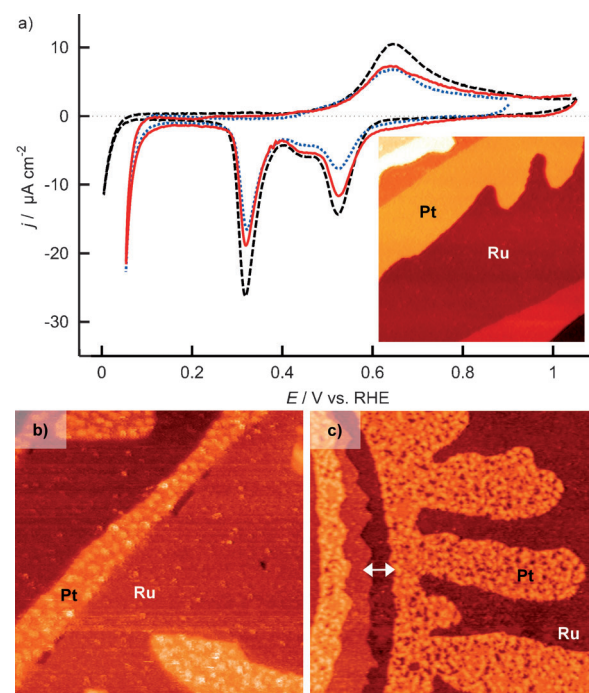 an irreversible modification of the adsorption/desorption current features in the CV (see the Supporting Information for further information).

Comparable measurements were performed on Pt-monolayer-island-modified Ru(0001) electrodes, using two different upper potential limits (0.9 V, 1.05 V). In Figure 2 a we show the CV (up to 0.9 V, blue dotted line) of a bimetallic Pt/Ru(0001) electrode with 0.32 monolayers (ML) of Pt deposited by physical vapor deposition in UHV (see the Supporting Information) and an STM image (inset) of the as-prepared surface. The STM image reveals a Pt-monolayer-thick stripe attached to the Ru steps, which extends along the lower Ru(0001) terrace. The CVs reveal a lower charge under the peak P3 compared to the bare Ru(0001) surface. Its charge (85 ± 2 μC cm^{-2}) is about 35 % less than that of pure Ru(0001), in good agreement with the Pt coverage determined by STM imaging. The images (Figure 2) also show that Pt losses during the electrochemical treatment are negligible. In contrast to Pt electrodeposition on Ru(0001), where a distinct hydrogen sorption region in the CV is observed,[12] we did not detect any features related to hydrogen sorption on the Pt monolayer deposits. We attribute this to the fact that H–Pt bonds on these sites are much weaker than those on bulk Pt surfaces.[13,14] The only indication for Pt on the surface, in addition to the change in charge in peak P3, is the shift in the onset potential of the H$_2$ evolution reaction by roughly 100 mV observed for the Pt-modified Ru(0001) surfaces. In contrast, the peak potentials for the other electrochemical processes remain unchanged, which indicates that Pt does not enhance the oxidation or reduction of the Ru(0001) surface.

Similar measurements performed on a 0.40 ML Pt modified Ru(0001) electrode after potential cycling in supporting electrolyte up to 1.05 V (red line, Figure 2a) exhibit identical electrochemical characteristics. However, the lower charge under peak P3 ($86 \pm 2 \, \mu C \, cm^{-2}$) points now to a Pt-free Ru(0001) area of 0.70 ML, which is in good agreement with the value determined from STM imaging after electrochemical measurements. Thus, either Pt loss or restructuring into clusters occurred upon potential cycling, which can however not be discerned by voltammetric measurements. Also for the two bimetallic surfaces the CVs are essentially identical, except for the increase in the peak P2 arising from the higher value of the upper potential limit.

Closer inspection of the STM images of the electrode surfaces after the electrochemical investigations (Figure 2b,c) shows large differences in their surface morphologies. After potential cycling up to 0.9 V, the monolayer-thick Pt structures along the Ru step edges remain intact and do not show any indication for Ru step edge corrosion, implying a stabilization by the attached Pt layer. In contrast, after potential cycling up to 1.05 V (Figure 2c), we find monolayer-deep holes along the former Ru step edges (see white arrows), indicating that under these conditions the Pt-induced stabilization no longer suffices to prevent corrosion of Ru step edges. From the smooth appearance of the Pt islands it is apparent that the large holes between the Pt islands and the newly formed Ru step arise from Ru removal. Furthermore, monolayer-deep holes within the Pt islands indicate that these are also affected by corrosion (see Figure 2c). Since the corrosion of the Ru terraces along the steps does not increase the exposed Ru area, the slight increase of the accessible Ru area upon cycling to high potential (see charge evaluation above) must be due to hole formation in the Pt monolayer deposit. It is important to keep in mind that in contrast to the considerable structural modifications detected by STM imaging, the CVs do not resolve any significant change in the electrochemical properties of these bimetallic surfaces.

Unequivocal effects of the potential-induced restructuring are visible, however, in the *I–E* traces for potentiodynamic bulk CO oxidation in Figure 3, which were recorded on the Pt-modified Ru(0001) samples after potential cycling to 0.90 V (blue dashed line) and 1.05 V (red dotted line), respectively. Here it is important to note that the surface morphology during CO electrooxidation is identical to that observed after the preceding potential cycling to the same upper potential limit; there are no indications for an additional, reversible restructuring upon immersion and emersion. Although we show the full cycle with its typical hysteresis, we will focus on the anodic scan in the following. Note also that Ru(0001) (black line) shows very little activity for CO electrooxidation throughout the entire potential range investigated. On both electrodes, CO oxidation is inhibited by CO_{ad} poisoning below 0.50 V, in agreement with previous findings.[14–16] The differences are particularly evident in the onset region between 0.50 V and 0.75 V (see Figure 3, inset).[17] For the non-restructured electrode (blue dashed line), the reaction starts at about 0.60 V in an approximately exponential way, while for the restructured surface cycled to 1.05 V (red dotted line) the onset of the reaction is shifted by
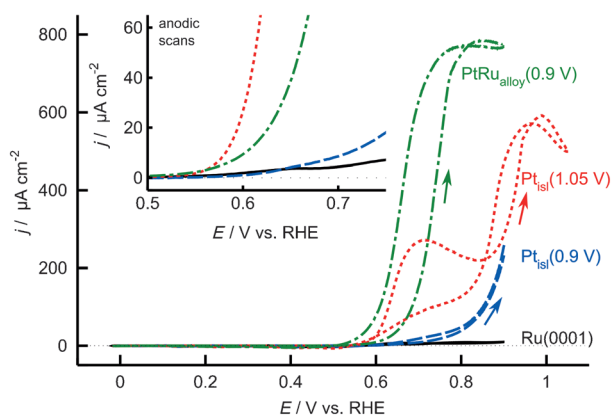

Figure 3. Potentiodynamic bulk CO oxidation in 0.5 M H_2SO_4 at 10 mVs^{-1} on Ru(0001) (black line), $Pt_{0.32-ML}$/Ru(0001) potential-cycled up to 0.9 V (blue dashed line), $Pt_{0.40-ML}$/Ru(0001) cycled up to 1.05 V (red, dotted line), and a $Pt_{0.3}Ru_{0.7}$/Ru(0001) surface alloy potential-cycled up to 0.9 V (green dashed-dotted line). Arrows indicate the anodic scan. The inset shows the low potential region at the onset of CO oxidation at higher magnification (anodic scans only).

almost 100 mV to lower potentials. In the latter case, the oxidation current first increases steeply, passes through a maximum at 0.67 V, and finally joins the potential current trace of the non-restructured sample. Hence, the structural modification invisible in the CV but clearly evident in the STM images, has a drastic effect in the CO oxidation behavior, leading to the appearance of a distinct prepeak.

For comparison, we also performed similar measurements on a $Pt_{0.3}Ru_{0.7}$/Ru(0001) monolayer surface alloy (green dash-dotted line) with an equivalent amount of surface Pt, which was also prepared under UHV conditions. The onset potential of this surface is similar to that of the restructured sample. In contrast to the restructured sample, however, the current increases continuously, making this the most active surface for potentials above 0.7 V.

Without knowing about the distinct restructuring of the Pt-island-modified Ru(0001) surface during the electrochemical measurements from STM imaging and the formation of new (defect) sites, one would have concluded that the enhanced catalytic activity between 0.50 and 0.80 V originates from bimetallic interfaces present at the Ru step with attached Pt and at the Pt island edges, which is exactly what would be expected from a bifunctional mechanism predicted for this reaction.[7] This argument would be further supported by the high activity of the PtRu/Ru(0001) surface alloy, which has an even higher number of bifunctional PtRu sites, and this was indeed concluded in former studies from the high activity of Pt-modified Ru electrodes in this potential region.[14, 17] The data presented in Figures 2 and 3 show, however, that these mechanistic conclusions are not correct, since for the non-restructured surface the activity remains rather low in this potential region; in other words, the RuPt sites present on these surfaces are not sufficient to cause a measurable increase in activity in this potential region.

Since one might argue that the lack of activity on the non-restructured surface is simply due to the low number of interface sites, as a result of the large size of the Pt islands, we

performed similar measurements on Pt-island-modified Ru-(0001) electrodes (with comparable Pt contents) where the number of PtRu sites is significantly higher, due to a higher density of much smaller Pt monolayer islands (see Figure 4, inset). I–E curves recorded after potential cycling to 0.90 V (Figure 4a, blue dashed line) show an onset potential of 0.60 V and an approximately exponential increase of the
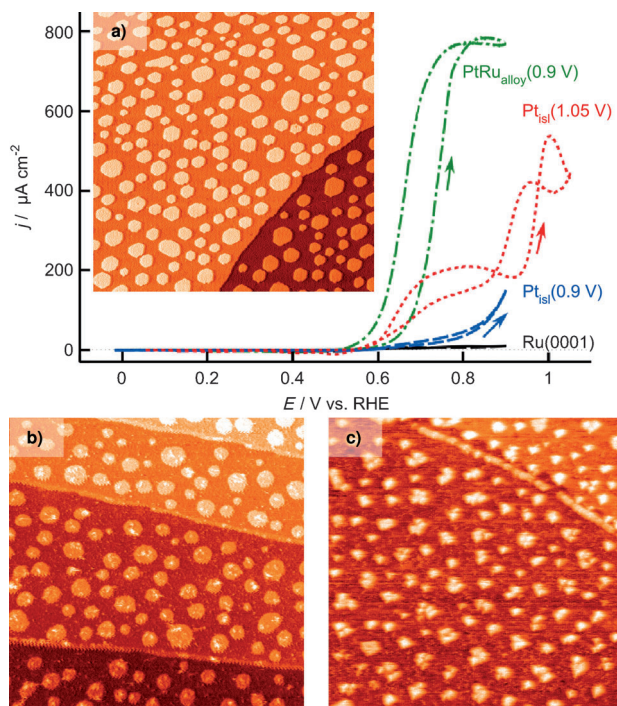
monolayer-modified Ru(0001) electrodes during the electrochemical treatment (or the formation of comparable structures upon in situ electrodeposition),[15,18] which evidently leads to highly active sites that have not yet been identified by STM, but which must be different from the edge sites of the monolayer Pt islands. The rather low activity of the non-restructured bimetallic surface is illustrated also by the onset potential for bulk CO oxidation which is essentially identical to that on Pt(111).[19]

In summary, using bulk CO oxidation on bimetallic PtRu model electrodes as an example, we have clearly demonstrated the necessity for detailed structural characterization of mono- and bimetallic model electrodes for an unambiguous mechanistic interpretation and for the proper identification of active sites on an atomic scale. We further demonstrated that potential-induced structural modifications of the bimetallic surface during the electrochemical and electrocatalytic processes, which may not be resolved in CVs because of the low concentration, can nevertheless severely modify or even dominate the catalytic behavior, an aspect which has been neglected in many previous studies on model surfaces and should receive more attention in the future.

Figure 4. a) Potentiodynamic bulk CO oxidation in 0.5 M H$_2$SO$_4$ at 10 mVs^{-1} on Ru(0001) (black line), Pt$_{0.29\text{-ML}}$/Ru(0001) potential-cycled up to 0.9 V (blue dashed line), Pt$_{0.39\text{-ML}}$/Ru(0001) cycled up to 1.05 V (red dotted line), and a Pt$_{0.3}$Ru$_{0.7}$/Ru(0001) surface alloy potential-cycled up to 0.9 V (green, dashed-dotted line). Arrows indicate the anodic scan. The inset shows the as-prepared electrode with 0.28 ML Pt deposited on Ru(0001) (200 nm × 200 nm). b,c) STM images (200 nm × 200 nm) of the electrodes after potential cycling up to 0.9 V (b) and 1.05 V (c).

oxidation current, with little activity in the potential range between 0.50 V and 0.80 V. STM images recorded before and after electrochemical measurements (Figure 4a inset and b) reveal that similar to our previous observations (Figure 2) the Pt coverage (0.29 ML) remains unchanged. Upon potential cycling to 1.05 V, the catalytic activity between 0.50 V and 0.80 V increases dramatically (Figure 4a, red dotted line), similar to our findings for the large Pt islands in Figure 3. This correlates to a severe restructuring of the small Pt islands, forming clusters up to four layers high and a dramatic increase in Pt-free Ru area, from 0.60 ML to 0.85 ML, which is illustrated in the STM image in Figure 4c.

The above data clearly demonstrate that PtRu sites at the edges of the Pt monolayer islands are not responsible for the strong enhancement of the CO oxidation activity in the potential range 0.50–0.80 V reported in earlier studies. Instead, it originates from the severe restructuring of the Pt-

[1] F. Maroun, F. Ozanam, O. M. Magnussen, R. J. Behm, *Science* **2001**, *293*, 1811–1814; L. A. Kibler, A. M. El-Aziz, R. Hoyer, D. M. Kolb, *Angew. Chem. Int. Ed.* **2005**, *44*, 2080–2084; *Angew. Chem.* **2005**, *117*, 2116–2120; J. Zhang, M. B. Vukmirovic, M. Mavrikakis, R. R. Adzic, *Angew. Chem. Int. Ed.* **2005**, *44*, 2132–2135; *Angew. Chem.* **2005**, *117*, 2170–2173; H. E. Hoster, M. J. Janik, M. Neurock, R. J. Behm, *Phys. Chem. Chem. Phys.* **2010**, *12*, 10388–10397; A. S. Bandarenka, et al., *Angew. Chem. Int. Ed.* **2012**, *51*, 11845–11848; *Angew. Chem.* **2012**, *124*, 12015–12018; F. Calle-Vallejo, M. T. M. Koper, A. S. Bandarenka, *Chem. Soc. Rev.* **2013**, *42*, 5210–5230; S. Brimaud, R. J. Behm, *J. Am. Chem. Soc.* **2013**, *135*, 11716–11719.
[2] N. P. Lebedeva, M. T. M. Koper, J. M. Feliu, R. A. van Santen, *Electrochem. Commun.* **2000**, *2*, 487–490.
[3] D. S. Strmcnik, D. V. Tripkovic, D. van der Vliet, K. C. Chang, V. Komanicky, H. You, G. Karapetrov, J. P. Greeley, V. R. Stamenkovic, N. M. Markovic, *J. Am. Chem. Soc.* **2008**, *130*, 15332–15339.
[4] O. A. Petrii, *J. Solid State Electrochem.* **2008**, *12*, 609–642.
[5] T. R. Ralph, *Platinum Met. Rev.* **2002**, *46*, 117–135.
[6] M. P. Hogarth, T. R. Ralph, *Platinum Met. Rev.* **2002**, *46*, 146–164.
[7] M. Watanabe, S. Motoo, *J. Electroanal. Chem.* **1975**, *60*, 275–283.
[8] N. S. Marinković, J. X. Wang, H. Zajonz, R. R. Adzic, *J. Electroanal. Chem.* **2001**, *500*, 388–394.
[9] J. X. Wang, N. S. Marinković, H. Zajonz, R. R. Adzic, *J. Phys. Chem. B* **2001**, *105*, 2809–2814.
[10] N. S. Marinkovic, M. B. Vukmirovic, R. R. Adzic in *Modern Aspects of Electrochemistry* (Eds.: C. Vayenas, R. White, M. Gamboa-Aldeco), Springer, New York, **2008**, pp. 1–52.

[11] M. B. Vukmirovic, R. L. Sabatini, R. R. Adzic, *Surf. Sci.* **2004**, *572*, 269 – 276.

[12] S. R. Brankovic, J. McBreen, R. R. Adzic, *J. Electroanal. Chem.* **2001**, *503*, 99 – 104.

[13] T. Diemant, T. Hager, H. E. Hoster, H. Rauscher, R. J. Behm, *Surf. Sci.* **2003**, *541*, 137 – 146.

[14] H. E. Hoster, R. J. Behm in *Fuel Cell Catalysis: A Surface Science Approach* (Ed.: M. T. M. Koper), Wiley, Chichester **2009**, pp. 465 – 505.

[15] S. R. Brankovic, N. S. Marinkovic, J. X. Wang, R. R. Adzic, *J. Electroanal. Chem.* **2002**, *532*, 57 – 66.

[16] O. B. Alves, H. E. Hoster, R. J. Behm, *Phys. Chem. Chem. Phys.* **2011**, *13*, 6011 – 6021.

[17] M. S. Rau, M. R. Gennero de Chialvo, A. C. Chialvo, *J. Power Sources* **2012**, *216*, 464 – 470.

[18] A. L. N. Pinheiro, M. S. Zei, G. Ertl, *Phys. Chem. Chem. Phys.* **2005**, *7*, 1300 – 1309.

[19] N. M. Markovic, P. N. Ross, Jr., *Surf. Sci. Rept.* **2002**, *45*, 117 – 229.